



AIMS Energy, 6(3): 402–413.

DOI: 10.3934/energy.2018.3.402

Received: 12 January 2018

Accepted: 25 April 2018

Published: 04 May 2018

<http://www.aimspress.com/journal/energy>

Technical note

A new NANOSATs propulsion system: swirling-combustion chamber and water electrolysis

Angelo Minotti^{1,2,*}¹ School of Aerospace Engineering, Sapienza University of Rome, Rome, Italy² Angelo Minotti ent., Rome, Italy* **Correspondence:** Email: angelo.minotti@uniroma1.it, info@angelominotti.com.

Abstract: Defined for academic purposes (low budget projects), NanoSats become of interest in the government and industry communities, since the deployment of swarms would be able to act as a single orbiting constellation, providing greater coverage and faster update rates than can be achieved using conventional single satellite operations. On the other hand, that accomplishment is hampered by the absence, due to the satellite's small dimensions, of an independent efficient propulsion system. This paper investigates the potentialities of a swirling-micropropulsion system that would permit NANOSATs to be "propulsive-independent". This would allow orbital operations, even at very low altitude, and/or increasing also life-times. The propulsion system, patent pending, adopts H₂/O₂ obtained by water electrolysis, a swirling combustion chamber and a sub-supersonic nozzle to optimize the thrust. The numerical combustion simulations, of the micro-thrust chamber, show that performances are impressive, in particular if compared to the dimensions, and this would be of benefit in fields such as intelligence, disaster monitoring, CBRNe observation, telecommunications and identification.

Keywords: swirling microcombustion chambers; water electrolysis; cubesats; nanosats; orbit changing; micropropulsion system; combustion simulations; H₂/O₂ detailed chemistry

1. Introduction

In 1999 [1] the California Polytechnic State University and the Stanford University developed a concept of satellite designed to utilize a standardised platform. Those satellites, known as

CubeSat (belonging to the nanosatellites family), are cubic modular satellites of “10 cm sides–1 kg weight” for each module/unit. Defined for academic purposes and necessities (low budget projects), a fundamental boost has been impressed by the MEMS fabrication technology (Micro Electrical Mechanical Systems), which has permitted components miniaturization [2]. Moreover, CubeSats become of interest in the government and industry communities, since the benefits of swarm satellite technologies have become more apparent [3]. A swarm of CubeSats would mean a group of dozens, up to hundreds, satellites able to act as a single orbiting constellation, providing greater coverage and faster update rates than can be achieved using conventional single satellite operations. That accomplishment is hampered by the absence of a CubeSat independent propulsion system. In fact, nowadays, most of the CubeSats operate in low Earth orbits determined by the deployment from the launch vehicle [4] and none have incorporated propulsion capable of substantial ΔV in order to extend their operability beyond Low Earth Orbit (LEO), or to orbits control, formation flying, proximity operations, fine attitude control, or lifetime extension and de-orbiting. To realize these manoeuvres, a propulsion system beyond the current state of the art is required. Such a propulsion system must be consistent with the CubeSats cost and mass-volume limitations. Attitude control is generally, roughly 60% of small satellites, addressed adopting magnetic control and only 9% of operational small satellites are equipped with an orbital control system [5] (the most popular being a cold gas propulsion system, therefore limited by low specific impulse, low impulse density propellants, low ΔV and thrust). Only one small satellite currently in orbit, as of 2010, has a chemical propulsion system [5]. Simultaneously, a high-pressure bi-propellant micro-rocket engine is already being developed [6] using MEMS technology. High-pressure turbopumps and valves are incorporated onto the rocket chip and a spark ignites the $\text{CH}_4\text{-O}_2$ mixture (the spark imposes chamber’s size limitation, because it cannot be shrunk proportionately with the thruster).

This combustor is of the order of centimetres with plans to operate at 12.7 MPa. Unfortunately, high operating pressures are not practical for nanosatellite systems.

Past [7] and actual [8] investigations try to solve those issues and/or to suggest solutions, even in the manufacturing technologies, but all of them present technical drawbacks and/or low performance and/or are not still ready to be mounted on satellites.

Notwithstanding those limits, a business analysis [9] foresees 2400 nano/microsatellites launches, within 2023, with a market of about 2 billion\$ only in the 2019.

In the light of the above, the present paper presents an innovative micro-propulsion system, patent pending [10], which adopts H_2/O_2 as fuel/oxidizer, obtained by water electrolysis and introduced into a micro-swirling combustion chamber (characteristic dimensions order of millimetres). The relative hot gases are expanded in a sub-supersonic nozzle to optimize the provided thrust.

Nowadays, there are examples, scientific and industrial (i.e., [11–13]), that show interest in miniaturized “electrolysis propulsion”, but none of them adopts swirling combustion chambers. This means that those thrust chambers, adopted in [11–13], are bigger than the swirling one reported in the present manuscript, with the final consequence of shorter operability or lower power per unit volume.

Therefore, the miniaturized propulsion system, here reported, tries to overcome the current nanosats’ limits, achieving orbit manoeuvres and lifetime extension, together with high combustion efficiency in extremely small dimensions.

The paper is structured as follows: section 2 reports the propulsion system's main technologies, section 3 reports the thrust chamber, section 4 reports the numerical/operating conditions and simulation results, while section 5 reports the conclusions.

2. The micro-propulsion system: main technologies

The innovative nanosatellite propulsion system merges 3 main technologies: electrolysis [8], a micro swirling combustion chamber and eventually catalysis [14]. In particular, liquid water is used as propellant and separated, by electrolysis, in H_2 - O_2 flows that are introduced into a swirling combustion chamber, eventually characterized by catalytic walls in order to ignite the mixture without sparks (or supporting the common spark ignition system). The aim is to overcome the actual nanosatellites limits and to extend significantly their fields of application and operability to CBRNe, intelligence analysis, disaster observation/prevention, climate analysis, planets observations-exploration and telecommunications.

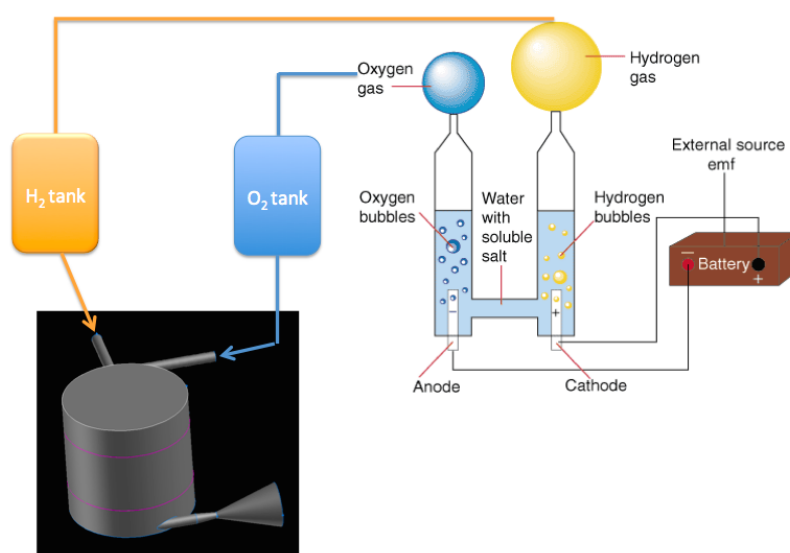


Figure 1. Micro propulsion system: overall structure, swirling chamber (left), electrolysis (right).

There are many benefits:

- (1) water is unpressurized and safe during launch, poses no risk to the rocket or primary payload, can operate in very low power modes, and leads to a relatively inexpensive system;
- (2) electricity for the electrolysis is generated by the solar cells (nominally 1.23 V are enough). Moreover, the propellant may serve as a battery, storing the electrical power with far greater mass efficiency and none of the electrical losses associated with batteries;
- (3) electrolysis provides gaseous hydrogen, fuel, and oxygen, oxidant, at stoichiometric conditions; this means obtaining the highest flame temperature and almost exclusively steam, as products of combustion;
- (4) swirling combustion chamber and catalytic walls would permit to overcome the limitations intrinsic of miniaturized chambers [15] (flame quenching, unstable combustion, low residence time and low combustion efficiency) and then to realize a combustion chamber of the order of

few millimetres with high combustion efficiency and, potentially, no-spark for the ignition. Hot products are then expanded in a sub-supersonic micro-nozzle to generate the required thrust (bipropellant thrusters, as opposed to monopropellant thrusters, offer higher specific impulse, I_{sp} , performances approaching 320–350 sec).

3. The thrust chamber

The miniaturized thrust chamber is composed of a cylindrical swirling combustion chamber and a micronozzle. The combustion chamber's dimensions, reported in the present study, are 6×6 mm ($D \times H$), the ducts have a diameter of 0.5 mm, while the micronozzle presents throat and exit radiuses respectively equal to 0.15 mm and 1 mm (area expansion ratio equal to about 49); see Figure 2.

The swirling motion is imposed by the inlet fluid dynamics, the oxidant duct, O_2 , is tangential to the cylindrical wall while the fuel duct, H_2 , is perpendicular. The higher oxygen kinetic energy, see section 4, pushes the fuel against the chamber wall forcing a helical path. The outlet duct, tangential to the chamber's wall, and positioned at its bottom, obliges the internal flow to create recirculation before passing through the nozzle [16]. All that increases, significantly, the residence time, mixing and providing very high combustion efficiency in very small devices [17]. In order to simplify the ignition system, up to completely remove it, and to stress the miniaturization process, catalytic material (i.e., platinum) can be deposited on the chamber's internal walls. Catalysis lowers the activation energy [18], required to ignite the hydrogen/oxygen mixing, permitting even smaller chamber's dimensions and maintaining complete combustion.

The thrust chamber presents no particular difficulties to be manufactured and can be scaled depending on the mission's design necessities and on the required performance. Such a small device (6×6 mm) may deliver thrust of the order up to $1 \div 10$ N (the upper limit is defined by the inlet velocities, which can be tuned modifying the operating pressure and the inlet section area).

The following section 4 reports the case of a thrust chamber that provides about 3×10^{-2} N.

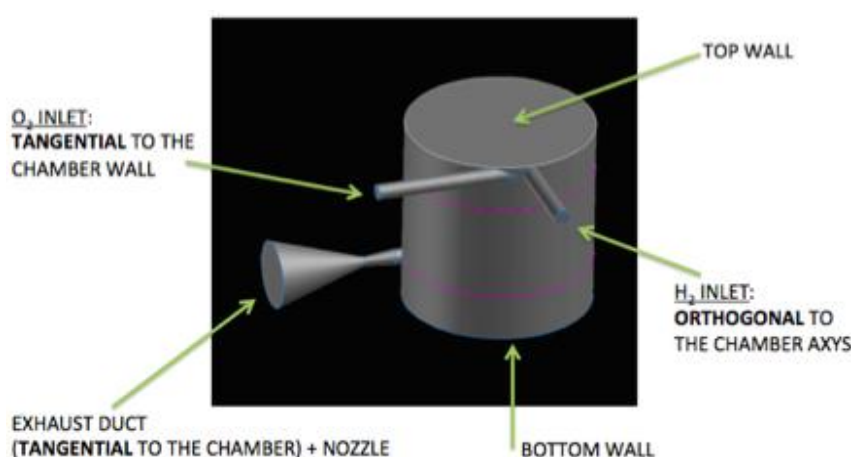


Figure 2. Rendering of the thrust chamber.

4. Numerical-operating conditions and results

The chamber, with a characteristic volume of $1.7 \times 10^{-7} \text{ m}^3$, has been reproduced by a mesh with 1.4 M cells (with a characteristic cell volume of $1.2 \times 10^{-13} \text{ m}^3$). It has been numerically improved by “reordering, smoothing, and swapping” techniques [19]. Fluid dynamics has been solved adopting the RANS k-eps turbulence approach, with the enhanced wall treatment [20]. The specific heat at constant pressure, C_{pi} , is fitted by polynomials of temperature [21], while viscosity and thermal conductivity, μ and k , are predicted by the gas kinetic theory [22]; mixtures are composition-dependent according to Wilke’s formula [23]. The turbulence-combustion coupling is modelled adopting the eddy dissipation concept (EDC) [24,25], while the hydrogen/oxygen kinetics by means of a detailed mechanism, 9 species and 21 reactions [26].

The reactive Navier–Stokes equations are solved adopting a finite-volume solver (Ansys 17 CFD code), the PISO scheme [27] (for the pressure-velocity coupling) and the third-order MUSCL scheme [28] (for the spatial discretization of all the variables). The computing resources are part of the CRESCO/ENEAGRID High Performance Computing infrastructure and its staff [29]. Simulation has been carried out assuming $8 \times 10^{-6} \text{ kg/s}$ and $1 \times 10^{-6} \text{ kg/s}$ of oxygen-hydrogen inlet mass flow rates and inlet pressure of 3 atm, see Figure 3. These conditions impose a kinetic energy ratio (oxygen kinetic energy/hydrogen kinetic energy) greater than 4.

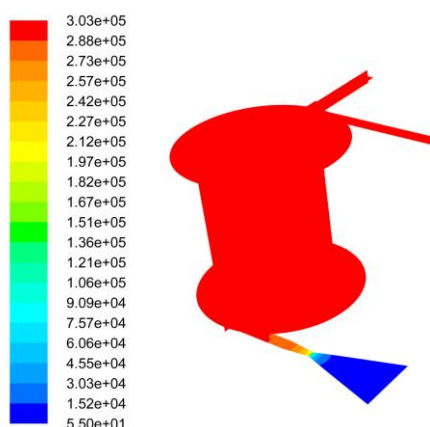


Figure 3. Pressure map, Pa.

All this, leads to laminar inlet Reynolds numbers (respectively 1000 and 400 for O_2 and H_2). Finally, walls have been assumed adiabatic, to mimic protective material (as it would be in the real case). Figures 4–5 report the internal temperature map and the zoom of the temperature at meeting points. The maximum temperature, in the core of the chamber, is about 3200 K, while the meeting point is characterized by a temperature close to 2400 K. Figures 6–7 report the velocity vectors at meeting points, coloured by temperature, and the map of the H_2 (fuel) mass fraction; it is evident how the impinging zone, between fuel and oxidizer, creates a “tongue”, characterized by a high temperature, close to 2400 K, that works as a premixing and ignition zone.

It has been previously reported that the main characteristic of the swirling chamber is the possibility

to miniaturize the system, maintaining high efficiency, thanks to the high recirculation and mixing levels.

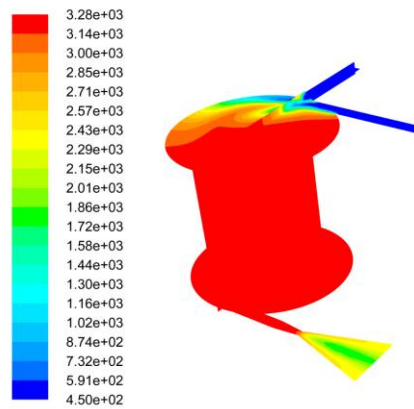


Figure 4. Temperature map, K.

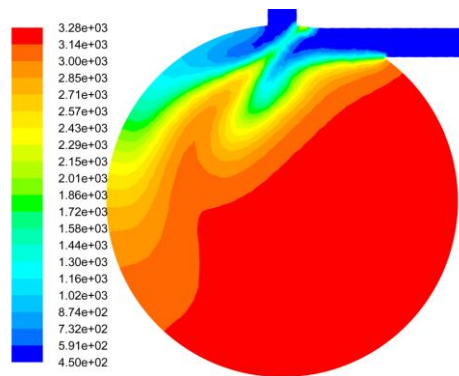


Figure 5. Zoom of the temperature map at the inlet plane, K.

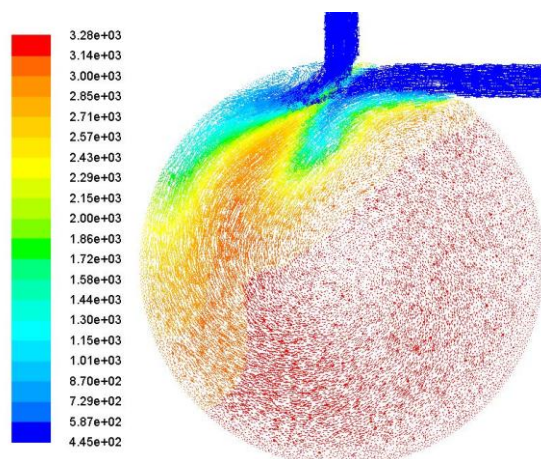


Figure 6. Zoom the velocity vectors, coloured by temperature, at inlet plane, K.

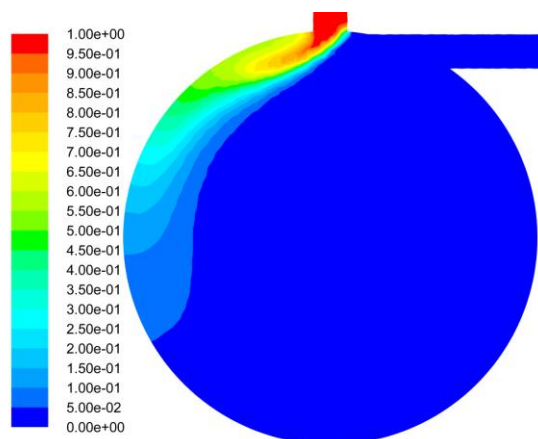


Figure 7. Zoom of the H₂ map at the inlet plane.

The following Figures 8–13 can prove all that. They report velocity vectors, velocity maps and velocity path lines. In particular, the velocity vectors, Figure 8, show how the oxidizer pushes the fuel against the wall, imposing swirling motion. This phenomenon is further highlighted by Figures 9–11, which show the velocity path-lines from, respectively, the oxidizer, the fuel inlets and their combination.

The helical path, vortexes and recirculation bubbles, just imposed by the inlet ducts relative position, increase the residence time allowing complete combustion in a very small device.

The final result is translated into the exhaust velocity values and, consequently, into the specific impulse, shown in Figures 12–13.

The exhaust velocity reaches values greater than 3300 m/s, with a specific impulse approaching 350 s, see Figures 12–13, and a thrust of about 3×10^{-2} N.

Optimized bell shaped nozzle and greater inlet flows, to increase the performance, are under investigations. Assuming 500 g of propellant and a lower specific impulse of 300 s, the thrust chamber provides a $\Delta V > 400$ m/s. This ΔV permits to form constellations at 200–300 km, from a 700 km deployment, and to extend the relative satellites' lifetime, according to mission requirements.

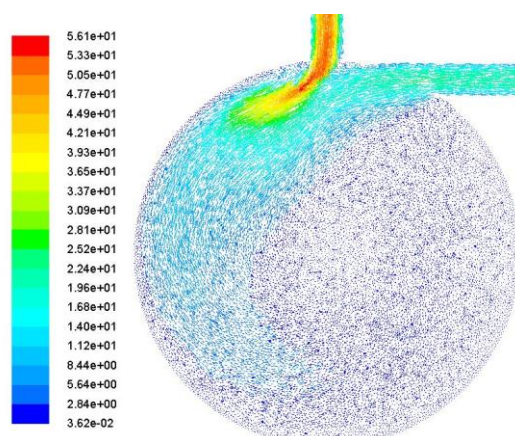


Figure 8. Velocity vectors at the inlet plane, m/s.

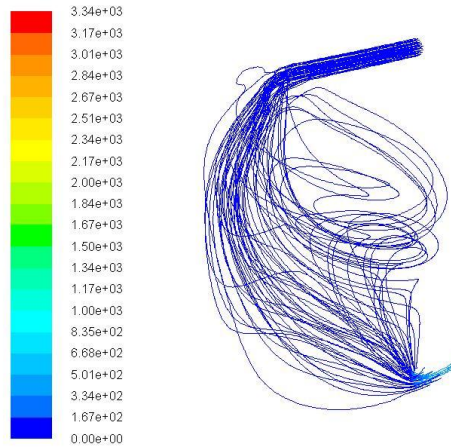


Figure 9. Velocity path lines from the O₂ inlet, m/s.

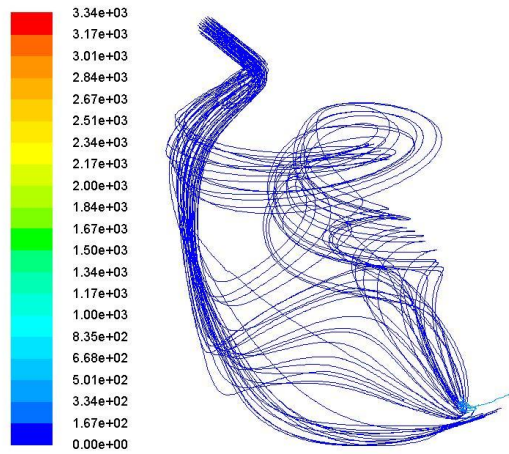


Figure 10. Velocity path lines from the H₂ inlet, m/s.

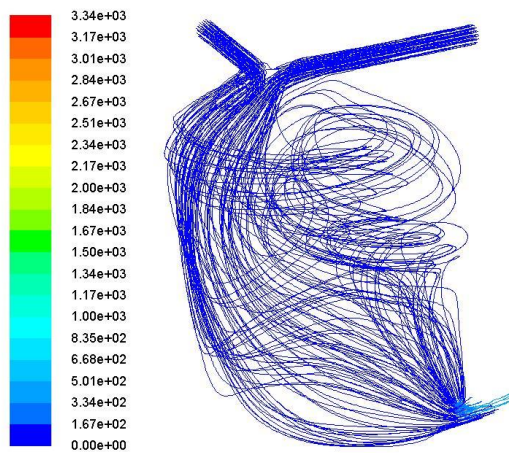


Figure 11. Velocity path lines from the O₂ and H₂ inlet, m/s.

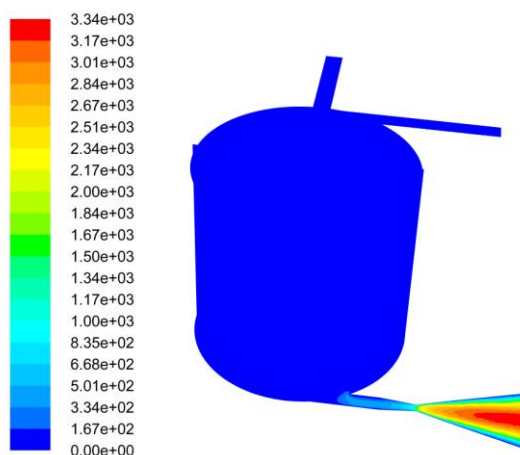


Figure 12. Velocity map, m/s.

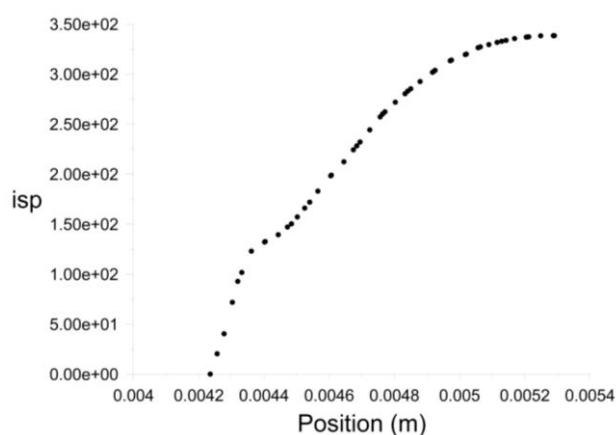


Figure 13. Isp, sec., along of the exhaust nozzle section's radius.

5. Conclusions

New satellite infrastructures (nanosats) are of interest for their low cost, easy of manufacturing and their potentialities to be deployed as swarms in order to act as a single orbiting constellation. That accomplishment, which would provide greater coverage and faster update rates than can be achieved using conventional single satellite operations, is hampered by the absence of an independent propulsion system that must be simultaneously enough small, efficient and performing. This manuscript presents an innovative miniaturized thrust chamber, fed by hydrogen and oxygen, obtained by electrolysis, patent pending, that would overcome the limits of the current solutions, permitting, therefore, both orbit constellations and fast manoeuvres. Even though the system is based on apparently simple technologies, it fulfils the following design requirements: miniaturized dimensions, high combustion efficiencies, scalability and high performance.

Outcomes are extremely promising; simulation and technical improvements may be done, respectively, adopting LES and an optimized bell shaped nozzle.

Conflict of interests

The author declares no conflict of interest in this paper.

References

1. Puig-Suari J (2014) CubeSat Design Specification. California Polytechnic State University, San Luis Obispo, rev. 13.
2. Yetter RA, Yang V, Aksay IA, et al. (2004) Meso and micro scale propulsion concepts for small spacecraft. Meso & Micro Scale Propulsion Concepts for Small Spacecraft. Available from: https://www.researchgate.net/publication/235181218_Meso_and_Micro_Scale_Propulsion_Concepts_for_Small_Spacecraft.
3. Verhoeven CJM, Bentum MJ, Monna GLE, et al. (2011) On the origin of satellite swarms. *Acta Astronaut* 68: 1392–1395.
4. Grieg AD (2015) Pocket Rocket: an electrothermal plasma microthruster. Ph.D. Thesis, Australian National University.
5. Bouwmeester J, Guo J (2010) Survey of worldwide pico- and nanosatellite missions, distributions and subsystem technology. *Acta Astronaut* 67: 854–862.
6. London AP, Epstein AH, Kerrebrock JL (2001) High-pressure bipropellant microrocket engine. *J Propul Power* 17: 780–787.
7. Groot DW, Oleson S (1996) Chemical microthruster options. NASA Contractor Report 198531.
8. Marshall WM, Stegeman JD, Zemba M, et al. (2013) Using Additive manufacturing to print a CubeSat propulsion system. 51st AIAA/SAE/ASEE Joint Propulsion Conference, Orlando, AIAA Propulsion and Energy Forum, (AIAA 2015-4184). Available from: <https://ntrs.nasa.gov/archive/nasa/casi.ntrs.nasa.gov/20150022181.pdf>.
9. Space Works (2017) Nano/Micro Satellite Market Forecast. Available from: http://spaceworksforecast.com/docs/SpaceWorks_Nano_Microsatellite_Market_Forecast_2017.pdf.
10. Minotti A (2017) Space propulsion system. Patent No: 102017000087235, filed.
11. Zeledon R (2015) Electrolysis propulsion for small-scale spacecraft. Ph.D Thesis, Cornell University.
12. Tethers Unlimited, Hydros. Available from: <http://www.tethers.com/HYDROS.html>.
13. Pothamsetti R, Thangavelautham J (2016) Photovoltaic electrolysis propulsion system for interplanetary CubeSats. Aerospace Conference. *IEEE*, 1–10.
14. Schneider S (2003) Catalyzed ignition of bipropellants in microtubes. NASA/TM-2003-21226, AIAA-2003-0674. Available from: <https://ntrs.nasa.gov/archive/nasa/casi.ntrs.nasa.gov/20030022776.pdf>.
15. Bruno C (2001) Chemical Microthrusters: Effects of Scaling on Combustion. AIAA 2001-3711, 37th AIAA/ASME/SAE/ASEE Joint Propulsion Conference, Salt Lake City, UT. Available from: https://www.researchgate.net/publication/236270204_Chemical_Microthrusters_Effects_of_Scaling_on_Combustion.
16. Minotti A, Teofilatto P (2015) Swirling combustor energy converter: H₂/Air simulations of separated chambers. *Energies* 8: 9930–9945.

17. Minotti A (2017) Hybrid energy converter based on swirling combustion chambers: The hydrocarbon feeding analysis. *AIMS Energy* 5: 506–516.
18. Appel C, Mantzaras J, Schaeren R, et al. (2004) Catalytic combustion of hydrogen–air mixtures over platinum: validation of hetero/homogeneous chemical reaction schemes. *Clean Air* 5: 21–44.
19. Cuthill EH, McKee J (1969) Reducing bandwidth of sparse symmetric matrices. In: Proceedings of the Association for Computing Machinery 24th National Conference, New York, NY, USA, 157–172.
20. Shih TH, Liou WW, Shabbir A, et al. (1995) A new k - ϵ eddy-viscosity model for high reynolds number turbulent flows. *Comput Fluids* 24: 227–238.
21. GRIMech 3.0 Thermodynamic Database. Available from: http://www.me.berkley.edu/gri_mech/version30/files30/thermo30.dat.
22. Anderson JD (1989) Hypersonic and high temperature gas dynamics. McGraw Hill: New York, NY, USA. 12: 468–481.
23. Mathur C, Saxena SC (1966) Viscosity of polar gas mixture: Wilke’s method. *Flow Turbul Combust* 15: 404–410.
24. Magnussen BF (1981) On the structure of turbulence and a generalized eddy dissipation concept for chemical reaction in turbulent flow. In: Proceedings of the 19th American Institute of Aeronautics and Astronautics Aerospace Science Meeting, St. Louis, MO, USA, 12–15.
25. Gran IR, Magnussen BF (1996) A numerical study of a bluff-body stabilized diffusion flame. Part 2. Influence of combustion modelling and finite-rate chemistry. *Combust Sci Technol* 119: 191–217.
26. Li J, Zhao Z, Kazakov A, et al. (2004) An updated comprehensive kinetic model of hydrogen combustion. *Int J Chem Kinet* 36: 566–575.
27. Ferziger JH, Perić M (1997) Computational methods for fluid dynamics. *Phys Today* 50: 80–84.
28. Vanleer B (1979) Toward the ultimate conservative difference scheme V. A second order sequel to godunov’s method. *J Comput Phys* 32: 101–136.
29. CRESCO: Centro computazionale di RicErca sui Sistemi Complessi. Available from: <http://www.cresco.enea.it/english>.



AIMS Press

© 2018 the Author(s), licensee AIMS Press. This is an open access article distributed under the terms of the Creative Commons Attribution License (<http://creativecommons.org/licenses/by/4.0>)